

The Relevance of Carbohydrate Hydrogen-Bonding Cooperativity Effects: A Cooperative 1,2-*trans*-Diaxial Diol and Amido Alcohol Hydrogen-Bonding Array as an Efficient Carbohydrate – Phosphate Binding Motif in Nonpolar Media

Eva Maria Muñoz,^[a] Manuela López de la Paz,^[a] Jesús Jiménez-Barbero,^[a] Gary Ellis,^[b] Marta Pérez,^[a] and Cristina Vicent^{*[a]}

Dedicated to Dr. Soledad Penadés on the occasion of her 60th birthday

Abstract: Carbohydrates with suitably positioned intramolecularly hydrogen-bonded hydroxyl and amide groups have the potential to act as efficient bidentate phosphate binders by taking advantage of σ - and/or σ,π -H-bonding cooperativity in nonpolar solvents. Donor–donor 1,2-*trans*-diaxial amido alcohol (**1**) and diol (**3**), in which one of the donor centres is cooperative, are very efficient carbohydrate–phosphate binding motifs. We have proven and quantified the key role of hydrogen-bonding centres *indirectly involved* in complexation,

which serve to generate an intramolecular H-bond (six-membered *cis* H-bond) in **1** and **3**. This motif enhances the donor nature of the H-bonding centres that are *directly involved* in complexation. A comparison of the thermodynamic parameters of the complexes formed between phosphate and a coop-

Keywords: carbohydrates • cooperative phenomena • hydrogen bonds • sugar–phosphate binding • supramolecular chemistry

erative (**1-Phos**) or anti-cooperative (**2-Phos**) bidentate H-bonded motif of a carbohydrate has allowed us to quantify the energetic advantage of H-bonding cooperativity in CDCl₃ and CDCl₃/CCl₄ (1:1.3) ($\Delta\Delta G^\circ = -2.2$ and -2.0 kcal mol⁻¹, respectively). The solvent dependences of the entropy and enthalpy contributions to binding provide a valuable example of the delicate balance between entropy and enthalpy that can arise for a single process, providing effective cooperative binding in terms of ΔG° .

Introduction

The carbohydrate moieties of some carbohydrate-containing antibiotics from microbial sources are responsible for the DNA groove binding and sequence selectivity of the drugs. 1,2- and 1,3-Sugar diols and amido alcohols of different relative configurations are structural motifs present in many of these compounds.^[1] Recent data have shown that the glycan chains alone are capable of giving rise to DNA sequence specificity^[2] and have suggested the presence of hydrogen bonds (H-bonds)^[3] between the carbohydrate and the phosphate backbone.^[4] The lack of knowledge on basic aspects

regarding the interactions responsible for the selectivity and specificity of carbohydrate–nucleic acid binding makes it difficult to effectively design new carbohydrate–DNA binders.^[5] We are exploring the use of carbohydrate hydrogen-bonding cooperativity as a tool to achieve binding of carbohydrates to the H-bonding motifs present in the grooves of DNA.^[6] We present herein our studies on the use of cooperativity in efficiently binding the hydrogen-bonding centres of a sugar derivative to the phosphate hydrogen-bonding motif, as well as an evaluation of its energetic contribution to binding in nonpolar solvents.

We have previously demonstrated that the rigid 1,3-*cis*-diaxial diol **1**, a 1,6-anhydro- β -D-glucopyranoside derivative, features a directional intramolecular O-H2 \rightarrow O-H4 H-bond. This generates a polarised bidentate donor–acceptor H-bonding element (Figure 1), which possesses enhanced donor (OH4) and acceptor (OH2) abilities.^[7] Diol **1** also bears an amide group at the 3-position of the pyranose ring, of which the NH is H-bonded to O1.^[8] Therefore, it presents a bidentate donor–donor 1,2-*trans*-diaxial amido alcohol (O-H4, N-H3) H-bonding motif. Molecular modelling studies have shown that a **1**–phosphate complex can be stabilised by

[a] Dr. C. Vicent, E. M. Muñoz, Dr. M. López de la Paz, Dr. J. Jiménez-Barbero, M. Pérez
Instituto de Química Orgánica General
CSIC, Juan de la Cierva 3, 28006 Madrid (Spain)
E-mail: iqocv18@iqog.csic.es

[b] Dr. G. Ellis
Instituto de Ciencia y Tecnología de Polímeros
CSIC, Juan de la Cierva 3, 28006 Madrid (Spain)

Supporting information for this article is available on the WWW under <http://www.wiley-vch.de/home/chemistry/> or from the author.

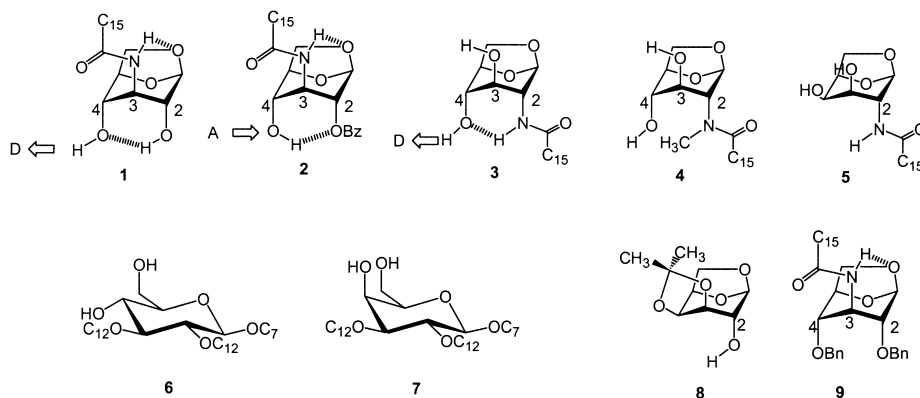


Figure 1. Carbohydrate derivatives **1–9** used in the binding studies.

bidentate hydrogen bonds.^[9] The 1,2-*trans*-diaxial amido alcohol **2**, a derivative of **1** with a benzoyl moiety in the 2-position, was selected as a further analogue of **1** to evaluate the effect of a cooperative acceptor hydroxyl centre (OH4) on phosphate binding. A stable intramolecular O-H4 → O2 H-bond has been characterised by IR in CH₂Cl₂ solution: **2** shows an OH stretching absorption at 3576 cm⁻¹ and no free OH band. This intramolecular H-bond should be broken in forming the bidentate intermolecular H-bond upon binding with the phosphate (anti-cooperative binding).

Compound **3** is a 1,2-*trans*-diaxial diol, the O-H4 of which forms part of a 1,3-*cis*-diaxial rigid amido alcohol motif, being an acceptor in a six-membered *cis* ring intramolecular H-bond (CON-H2 → O-H4)^[8] (Figure 1). The 1,2-*trans*-diaxial diol **4** and the 1,2-*cis*-diol **5** were synthesised as models of **3** that lack the aforementioned intramolecular six-membered-ring H-bond, either as a result of methylation of the amide NH (in **4**) or due to the different configuration of the 4-hydroxyl group on the pyranose ring (in **5**). Additionally, two flexible 1,3-diols involving the 4- and 6-positions of glucose (**6**) and galactose (**7**) were prepared to evaluate the effect of conformational flexibility in a 1,3-diol H-bonding motif on phosphate binding. The monoalcohol (**8**) and monoamide (**9**) were used as models of single interaction centre motifs.

Results and Discussion

Binding studies and structural characterisation: The complexation was studied by means of NMR spectroscopy in [D]chloroform. The sugars **1–9** (0.1–0.9 mM) were titrated with the phosphate [tetrabutylammonium bis(3,5-di-*tert*-butyl)phenyl phosphate, **Phos**] (1–9 mM), as described in the Experimental Section.^[10]

The stability constants and ΔG° values of the complexes of **1–5** and **7** with **Phos** are given in Table 1.^[11] The 1:1

Table 1. K_s and ΔG° values for the interaction between the carbohydrate derivatives **1–5** and **7** and the phosphate salt.

	1	2	3	4	5	7
K_s [M ⁻¹] ^[a]	4160	93	1796	1211	554	111
ΔG° [kcal mol ⁻¹] ^[b]	-4.9	-2.7	-4.4	-4.2	-3.7	-2.8

[a] $T = 298$ K, [D]chloroform. [b] Estimated error: ± 0.1 kcal mol⁻¹.

stoichiometries of all the phosphate complexes were determined by Job plots and Scatchard plots based on the chemical induced shifts.^[12] The most stable complexes proved to be **1-Phos** and **3-Phos**, with ΔG° values for binding of -4.9 and -4.4 kcal mol⁻¹, respectively. These measured energy values are larger than would be expected for a complex stabilised by a single or even by two charged H-bonds.^[13] Even more relevant, complex **2-Phos** is

-2.3 kcal mol⁻¹ less stable than **1-Phos**. The model derivatives, monoalcohol **8** and monoamide **9**, did not interact under the same conditions. This gives an indication of the cooperative nature of the H-bonding mediated interaction in **1-Phos** and **3-Phos**.

Comparison of the chemical induced shifts (CIS) and the temperature coefficients of the resonances of the exchangeable protons (OHs and NHs) measured for the free sugars and for the complexes (Tables 2 and 3) allowed the identification of the H-bonding centres involved in complexation. We found differences of one order of magnitude between the $\Delta\delta/\Delta T$ values of the OH resonances of the free ligand and those of the complexes in the case of **1**, **3**, **4**, and **5**. These resonances also showed the largest chemical induced shifts (-1.3 to -3.2 ppm) upon complexation. These facts clearly point to the involvement of these hydroxyls in an intermolecular H-bonding mediated process. This event could be mediated either by "direct involvement" in the intermolecular H-bonds

Table 2. CIS^[a] and $\Delta\delta/\Delta T$ ^[b] of the OH resonances of the carbohydrates **1**, **3**, **4**, and **5** in the free state and bound to the phosphate.

Compound	Resonance	CIS	$\Delta\delta/\Delta T$ (free) ^[c]	$\Delta\delta/\Delta T$ (bound) ^[d]
1	OH-2	+2.68	-2.4	-28.8
1	OH-4	+2.91	-4.3	-32.5
3	OH-3	+2.69	-2.1	-24.1
3	OH-4	+3.23	-1.6	-26.6
4 ^[e]	OH-3	+3.03	-3.7	-21.4
4 ^[e]	OH-4	+3.18	-5.7	-22.3
5	OH-3	+1.76	-3.1	-23.3
5	OH-4	+1.26	-8.7	-14.3

[a] CIS: $\delta_{\text{bound}} - \delta_{\text{free}}$, measured at 298 K. [b] ppb K⁻¹, measured in the range $T = 296 - 318$ K. [c] [sugar] = 1.0×10^{-4} M. [d] [sugar] = 1.0×10^{-4} M (**1-Phos** = 1:7.5) (**3-Phos** = 1:30) (**4-Phos** = 1:7.5) (**5-Phos** = 1:30). [e] OH-3 and OH-4 resonances are not unambiguously assigned.

Table 3. CIS^[a] and $\Delta\delta/\Delta T$ ^[b] of the NH resonances of the sugars **1**, **3**, and **5** in the free state and bound to the phosphate.

Compound	CIS	$\Delta\delta/\Delta T$ (free) ^[c]	$\Delta\delta/\Delta T$ (bound) ^[d]
1	+1.72	-1.2	-24.1
3	+0.38	-1.5	-4.3
5	+0.06	-2.3	-2.9

[a] CIS: $\delta_{\text{bound}} - \delta_{\text{free}}$, measured at 298 K. [b] ppb K⁻¹, measured in the range 296–318 K. [c] [sugar] = 1.0×10^{-4} M. [d] [sugar] = 1.0×10^{-4} M (**1-Phos** = 1:7.5) (**3-Phos** = 1:30) (**5-Phos** = 1:30).

with phosphate, or by “indirect involvement”, in other words, by taking part in an intramolecular H-bond that generates a cooperative H-bonding network upon complexation.^[6, 14] In contrast, there is notably different behaviour among the NH resonances of the sugars upon complexation (Table 3). Whilst the amide NH resonance parameters for **1** show large variations between the free and the bound state, the analogous resonance data for **3** show only small differences. Moreover, no changes are observable in the case of **5**. These experimental observations are consistent with the involvement of the amide NH of the sugar ligands in the complexation process, either “directly” as in the complex with **1** or “indirectly” as in that with **3**, whereas the amide NH is evidently not involved in the interaction with **5**.

Difference NOE and NOESY experiments on the free ligand **1**, and the sugar–**Phos** complex (**1-Phos**, 1:3 and 3:1 molar ratios) were performed in order to obtain structural information. NOE peaks supporting the presence of the ion pair^[15] in the complex were detected, but no intermolecular NOEs between the sugar resonances and the phosphate salt protons were observed. An intramolecular NOE (NH–H6_{endo}) was observed in the free sugar **1**, which disappeared upon bonding to the phosphate; this suggests a conformational change upon complexation, whereby the amide proton becomes directed towards the phosphate anion to establish the bidentate coordination (see Figure 2).

Additional structural information was provided by IR spectroscopy. The FT-IR spectra of sugars **1–7** (1 mM) and **Phos** (1–7 mM) were compared with those of the complexes sugar–**Phos** (1:1, 1:5, and 1:7 molar ratios)^[16] at a fixed concentration of the free component. The intensity of the absorptions attributable to the hydroxyls present in the free sugars ($\tilde{\nu}(\text{OH})_{\text{free}}$ and $\tilde{\nu}(\text{OH})_{\text{intra}} = 3597\text{--}3540\text{ cm}^{-1}$) decreased upon increasing the concentration of the phosphate. In each case, a broad band at $3400\text{--}3100\text{ cm}^{-1}$, attributable to intermolecular stretching absorptions ($\tilde{\nu}(\text{OH})_{\text{bound}}$ and/or $\tilde{\nu}(\text{NH})_{\text{bound}}$), appeared in the spectrum. Unfortunately, no differences in the behaviour of the $\tilde{\nu}(\text{OH})$ bands were found that would have allowed discrimination between direct or indirect binding of the hydroxyl groups. However, in accordance with the NMR behaviour of those sugar–**Phos** complexes in which an amide NH group can take part in binding (**1**, **3**, and **5**), there is clearly a difference in behaviour of the $\tilde{\nu}(\text{NH})$ stretching vibrations and of the characteristic amide I and II modes.^[17] In the case of **1-Phos**, $\tilde{\nu}(\text{NH})_{\text{free}}$ decreases in intensity and a $\tilde{\nu}(\text{NH})_{\text{bound}}$ absorption appears in the intermolecular region. Both amide bands, (I) and (II), showed the same behaviour, in agreement with a direct involvement of the NH in complexation. In contrast, in the case of **5**, no modification of the bands was observed for any of the relevant

absorptions, as expected for the non-involvement of the amide in the intermolecular process. Particularly relevant was the different behaviour of the **3-Phos** complex. In this case, the three amide absorptions corresponding to the unbound sugar showed small shifts upon increasing addition of **Phos**. The $\tilde{\nu}(\text{NH})_{\text{intra}}$ band was shifted from 3427 cm^{-1} in **3** to 3417 cm^{-1} in **3-Phos** (1:7), the amide (I) band from 1672 to 1664 cm^{-1} , and the amide (II) band from 1507 to 1512 cm^{-1} . These data indicate a strengthening of the intramolecular CON–H2 \rightarrow O–H4 bond^[18] by intermolecular cooperativity and are consistent with the proposed “indirect cooperative involvement” of the amide group of **3** (Figure 2) in the intermolecular process.

Unequivocal proof of the existence of the intramolecular H-bond O–H2 \rightarrow O–H4 in the **1-Phos** complex was provided by ^1H NMR partial deuteration experiments on this complex in $[\text{D}]\text{chloroform}$.^[19] Addition of microliter quantities of $[\text{D}_4]\text{methanol}$ to a 1:3 mixture of **1** and **Phos** (2.5 mM:7.5 mM, 93 % saturated) led to the appearance of an additional OD \cdots OH isotopomer signal (doublet) for each hydroxyl resonance (Figure 3), unambiguously confirming their involvement in intramolecular H-bonding.

The structural evidence provided by both ^1H NMR and IR spectroscopies clearly indicates that the cooperative 1,2-*trans*-diaxial amido alcohol or diol H-bonding motifs of sugars **1** and **3** are very efficient hydrogen-bonded bidentate donor–donor structural elements for phosphate binding (Figure 2) in non-polar solvents. Furthermore, the efficiency of the binding decreases significantly for the anti-cooperative 1,2-*trans*-diaxial amido alcohol **2** ($K_a = 93\text{ M}^{-1}$), which presents the same 1,2-*trans* bidentate hydrogen-bonding motif as **1** ($K_a = 4160\text{ M}^{-1}$), but in which the hydroxyl (OH4) is not a cooperative H-bonding donor centre (Figure 1). Thus, the most favourable binding motif is not based purely on a bidentate 1,2-*trans*-diaxial amido alcohol. Clearly, the cooperative donor nature of O–H4 in **1** further contributes to the association, and the six-membered-ring intramolecular H-bond is probably responsible for the cooperative complex stabilisation.

In order to evaluate the contribution of cooperativity to binding in the case of **3-Phos**, compounds **4** and **5** were prepared and phosphate complexation was studied. Unfortunately, ^3J values measured for the pyranose ring proton resonances of **4** in the free state showed that this compound exhibits a chair/boat equilibrium in CDCl_3 .^[20] Since the distance between the 1,2-*trans*-diol hydrogen-bonding centres varies depending on this conformational equilibrium, **4** does not provide a good model for evaluating the contribution of cooperativity to **3-Phos** stability. Nevertheless, the data in Table 1 show that **4-Phos** is a very stable complex, indicating

that **4** presents good complementarity with **Phos** in terms of distances. All structural parameters are in accordance with the participation of both hydroxyls in complexation. Moreover, comparison of this stability constant with that found for a 1,2-*trans*-cyclohexanediol bearing

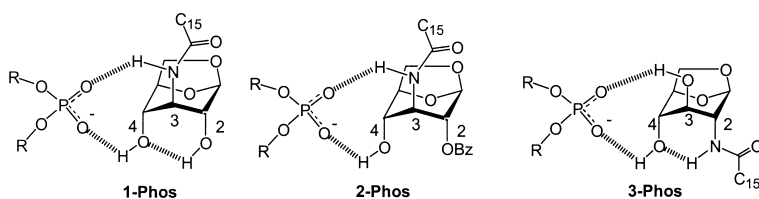


Figure 2. Schematic representations of complexes **1-Phos**, **2-Phos**, and **3-Phos** based on structural data from ^1H NMR and IR studies.

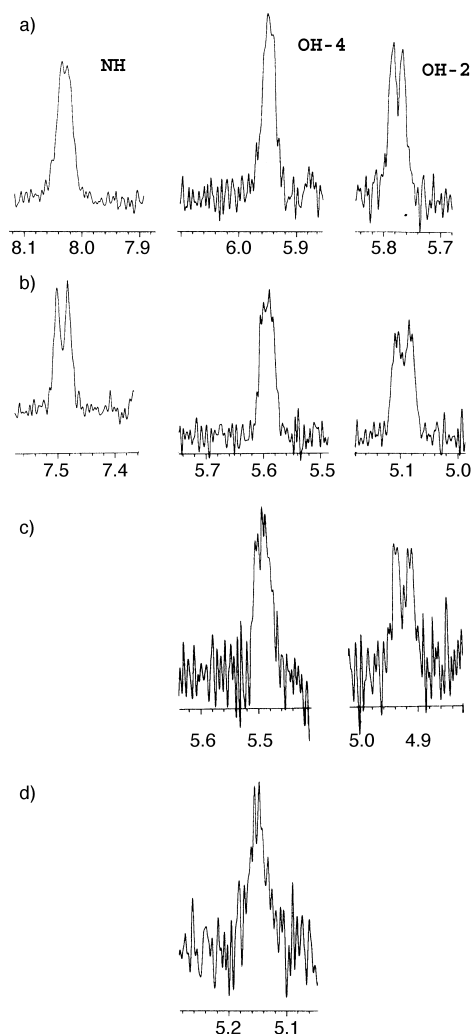


Figure 3. OH and NH proton resonances in ^1H NMR spectra of the complex **1-Phos** in CDCl_3 showing increasing levels of deuteration upon addition of $[\text{D}_4]\text{methanol}$: a) 0 %, b) 48 %, c) 75 %, d) 80 % in O-H4 (O-H2 has been fully deuterated in d).

equatorial vicinal OH groups,^[4b] 15.6M^{-1} , is particularly relevant and again suggests that the origin of the efficient binding is a good complementarity. The structural characterisation of **5-Phos** revealed the non-participation of the NH in binding and the involvement of both OHs in complexation with the phosphate.^[21] This fact suggests that the change in configuration of OH-4 from axial (**3**) to equatorial (**5**) induces a drastic change in the binding mode. Diol **7**, in which the distance between the H-bonding centres could be adjusted to that in **Phos**, also showed a small degree of binding (see Table 1) compared with **1** and **2**.

Thermodynamic parameters of the sugar–phosphate binding—Cooperativity contribution: Thermodynamic parameters of the complexes formed by **1**, **2**, and **3** with **Phos** were evaluated from the van't Hoff plots of the K_a values measured in CDCl_3 and $\text{CDCl}_3/\text{CCl}_4$ (1:1.3) by ^1H NMR at different temperatures (Table 4). In CDCl_3 , the most stable H-bonding motif is the bidentate cooperative H-bond present in **1-Phos** ($\Delta H^\circ = -13.6\text{ kcal mol}^{-1}$). The energetic contribution (ΔH°)

Table 4. Thermodynamic parameters for the interaction between the phosphate and the carbohydrate derivatives **1–3** in CDCl_3 and $\text{CDCl}_3/\text{CCl}_4$.

	K_a [M^{-1}] ^[a]	ΔG° [kcal mol^{-1}] ^[b]	ΔH° [kcal mol^{-1}]	$T\Delta S$ [kcal mol^{-1}] ^[a]
CDCl_3				
1	4160	−4.9	−13.6	−8.8
2	93	−2.7	−7.4	−4.8
3	1796	−4.4	−5.3	−0.8
$\text{CDCl}_3/\text{CCl}_4$				
1	7112	−5.3	−6.7	−1.4
2	237	−3.3	−10.5	−7.3
3	7649	−5.3	−5.8	−0.5

[a] $T = 298\text{ K}$. [b] Estimated error: $\pm 0.1\text{ kcal mol}^{-1}$.

of the two H-bonds that stabilise **1-Phos** (a cooperative 1,2-*trans*-diaxial amido alcohol) is $-8.3\text{ kcal mol}^{-1}$ greater than that in **3-Phos** (a cooperative 1,2-*trans*-diaxial diol). However, the value of ΔG° is similar for both complexes due to the large difference in the entropy term for the respective complexes ($-29.4\text{ cal mol}^{-1}\text{ K}^{-1}$ for **1-Phos** and $-2.8\text{ cal mol}^{-1}\text{ K}^{-1}$ for **3-Phos**). This difference indicates that the entropy cost of preorganisation upon complex formation is higher for **1-Phos** than for **3-Phos**. This is probably a consequence of the change of conformation about the CH–NH₃ bond, as suggested by the differences in the observed NOEs of **1** on going from the free to the bound state. The change is in accordance with cleavage of the intramolecular H-bond N–H3 \rightarrow O1 and the formation of a bidentate intermolecular H-bond with **Phos**. Additionally, the directionality of the intramolecular H-bond N–H2 \rightarrow O–H4 is more fixed in **3** than that of the intramolecular H-bond O–H2 \rightarrow O–H4 in **1**.^[22]

Complementarity in terms of distances of the 1,2-*trans*-bidentate motif with **Phos** also has to be taken in account. In this sense, comparison between **3-Phos** and **4-Phos** (**4-Phos**: $\Delta H^\circ = -6.3\text{ kcal mol}^{-1}$ and $\Delta S = -6.9\text{ cal mol}^{-1}\text{ K}^{-1}$) proved useful. ΔH° in **4-Phos** is 1 kcal mol^{-1} more favourable than that in **3-Phos**, even though there is a cooperative H-bonding network in the latter. This fact again suggests a better complementarity of distances between the H-bonding centres in **4-Phos**. However, **4-Phos** is less stable than **3-Phos** in terms of ΔG° , due to a worse entropy of binding. The system thus provides a typical example of enthalpy-entropy compensation.

To evaluate the contribution of cooperativity to the thermodynamics of binding of the cooperative 1,2-*trans*-diaxial amido alcohol, the data for the binding motif present in **1-Phos** were compared with those measured for the **2-Phos** complex. The **1-Phos** complex, with OH4 being a cooperative donor in the free sugar **1**, is $-6.2\text{ kcal mol}^{-1}$ ($\Delta\Delta H^\circ$) more stable than the anti-cooperative 1,2-*trans*-diaxial amido alcohol present in the **2-Phos** complex, with OH4 being a cooperative acceptor in the free state. Also, the formation of a cooperative intermolecular H-bonding network in **1-Phos** provides an additional stabilisation of $-2.2\text{ kcal mol}^{-1}$ ($\Delta\Delta G^\circ$). The highly unfavourable entropic term found for **2-Phos** is consistent with the fact that the stable intramolecular H-bond O–H4 \rightarrow O2 present in the amido alcohol

in the free state first has to rearrange in order to match the bidentate intermolecular H-bond with **Phos** (Figure 2).

Thermodynamic parameters of the complexes formed by **1**, **2**, and **3** with **Phos** were also determined in a $\text{CDCl}_3/\text{CCl}_4$ (1:1.3) mixture (Table 4). The stabilities of the three complexes in the nonpolar mixture were higher than those of the corresponding complexes in chloroform. However, the contributions of entropy and enthalpy to the overall binding were found to be very different. The values reflect the difficulty of maximising complementarity with the bidentate H-bonding motif in **Phos** and the influence of the intramolecular H-bond directionality depending on the solvent polarity.

The contribution of the cooperativity to the energy of binding ($\Delta\Delta G^\circ$, **1-Phos** versus **2-Phos**) was found to be similar in both media, -2.2 and $-2.0 \text{ kcal mol}^{-1}$ in CDCl_3 and $\text{CDCl}_3/\text{CCl}_4$, respectively.^[23] Despite the similarity, cooperativity in CDCl_3 is enthalpically driven ($\Delta\Delta H^\circ = -6.2 \text{ kcal mol}^{-1}$) whereas in $\text{CDCl}_3/\text{CCl}_4$ it is entropically driven ($T\Delta\Delta S = -5.9 \text{ kcal mol}^{-1}$) (Table 5). In both cases, cooperativity leads to an enthalpy–entropy balance that results in effective binding.

Table 5. Comparison of the thermodynamic parameters of **1-Phos** and **2-Phos** complexes in CDCl_3 and $\text{CDCl}_3/\text{CCl}_4$.

(1-Phos) – (2-Phos)	$\Delta\Delta G^\circ$ [kcal mol ⁻¹]	$\Delta\Delta H^\circ$ [kcal mol ⁻¹]	$T\Delta\Delta S$ [kcal mol ⁻¹] ^[a]
CDCl_3	-2.2	-6.2	$+4.0$
$\text{CDCl}_3/\text{CCl}_4$	-2.0	$+3.8$	-5.9

[a] $T = 298 \text{ K}$.

Conclusion

We have shown that H-bonding cooperativity can be an efficient tool for achieving carbohydrate–phosphate binding in nonpolar media. Sugars with suitably positioned intramolecularly hydrogen-bonded hydroxyl and amide groups have the potential to act as efficient bidentate phosphate binders by taking advantage of σ - and/or σ,π -H-bonding cooperativity.

The donor–donor 1,2-*trans*-diaxial amido alcohol (**1**) and diol (**3**), in which one of the donor centres is cooperative, are very efficient phosphate-binding motifs.

We have proven and quantified the key role of the hydrogen-bonding centres “indirectly involved” in complexation, which serve to generate an intramolecular six-membered *cis* H-bond in **1** and **3**, thereby enhancing the donor nature of H-bonding centres that are “directly involved” in complexation (O–H4).

A comparison of the thermodynamic parameters of the complexes formed between phosphate and cooperative (**1-Phos**) or anti-cooperative (**2-Phos**) bidentate H-bonded motifs of carbohydrates has allowed us to quantify the energetic advantage of H-bonding cooperativity in CDCl_3 and $\text{CDCl}_3/\text{CCl}_4$ (1:1.3) ($\Delta\Delta G^\circ = -2.2$ and $-2.0 \text{ kcal mol}^{-1}$, respectively).

The presented solvent-dependence analysis of the entropy and enthalpy contributions to binding provides an illustrative

example of the delicate balance between entropy and enthalpy that can exist for a single process. Enthalpy–entropy compensation phenomena have been shown to be operative.

Experimental Section

Compounds and solvents: Carbohydrate derivatives **1–9** and the phosphate salt (**Phos**) were prepared as described below, dried under high vacuum, and heated overnight at 40°C in the presence of P_2O_5 prior to the ^1H NMR and FT-IR experiments. All ^1H NMR studies were performed using freshly prepared solutions in $[\text{D}]\text{chloroform}$, which was always passed through basic alumina prior to use and stored over 4 \AA molecular sieves. The alumina and molecular sieves employed were freshly activated by heating at 600°C under high vacuum. All FT-IR experiments were carried out using freshly prepared solutions in CH_2Cl_2 , which was distilled and dried according to conventional methods and stored over 4 \AA molecular sieves under argon atmosphere.

^1H NMR experiments: The binding abilities of compounds **1–9** to **Phos** were investigated by means of ^1H NMR titration experiments. Carbohydrate solutions were obtained by diluting a known volume of a stock solution, previously prepared by dissolving a weighed amount of the sugar in $[\text{D}]\text{chloroform}$, to 3 mL . Then, 0.5 mL of the resulting solution was placed in an NMR tube and the remaining 2.5 mL were used to prepare the sugar/phosphate titrant solution. The carbohydrate concentrations were in the range 10^{-4} M to $9 \times 10^{-4} \text{ M}$, depending on the propensity for self-association of the particular carbohydrate. The concentration of **Phos** in the titrant solution was in the range 10^{-3} M to $9 \times 10^{-3} \text{ M}$. A minimum of 14 aliquots of the sugar/phosphate solution were added to the sugar solution, and a one-dimensional ^1H NMR spectrum ($T = 298 \text{ K}$) was recorded after each addition. The experiments were carried out at least in duplicate. The binding constants were evaluated from a least-squares fitting, using a well-established protocol.^[25] The $(\Delta\delta/\Delta T)$ values of the exchangeable proton resonances of compounds **1–7** and the respective complexes with **Phos** were obtained by means of variable-temperature ^1H NMR experiments. These were carried out at sugar concentrations ranging from 10^{-4} M to $5 \times 10^{-4} \text{ M}$, again depending on the propensity for self-association of the carbohydrate investigated, and the degree of saturation ranged from 60 to 85% in the complexes with **Phos**. Six spectra were recorded at different temperatures in the range $297–318 \text{ K}$ and $\Delta\delta/\Delta T$ values were evaluated from a linear fit.

Partial deuteration experiments: The **1-Phos** complex (**1-Phos** = 1:3, 93% saturation, $[\text{D}]\text{chloroform}$) was partially deuterated by adding a few microlitres of $[\text{D}_4]\text{methanol}$ to the NMR sample at 295 K . After each addition, a one-dimensional ^1H NMR spectrum was recorded and the deuteration percentage was calculated by comparison of the integrals of the resonances of the exchangeable protons (OH and NH resonances) with that of a non-exchangeable proton (such as H-1). Isotopic effects were observable for both OHs (signal doubling), demonstrating the existence of the intramolecular H-bond between the two OH groups in the complex. The NH did not exhibit signal doubling after deuteration.

FT-IR experiments: Carbohydrate solutions were prepared by dissolving a weighed amount of sugar in dry CH_2Cl_2 . Carbohydrate/phosphate solutions were prepared by dissolving a weighed amount of phosphate in the aforementioned carbohydrate solutions. Spectra were recorded at concentrations at which intermolecular H-bonding was negligible, on Nicolet 520 B or Perkin–Elmer spectrometers using liquid cells (KBr windows) of pathlength 0.1 mm . Background spectra were recorded with the neat solvent in the cell. This inevitably led to saturation in several regions of the spectra due to the solvent, but a clear spectral window down to around 3100 cm^{-1} was available. The spectral data were analyzed using Spectrum (Perkin–Elmer) software. In the estimation of peak frequencies, simple peak-picking (estimated bandhead maximum) was employed.

Molecular modelling: Molecular mechanics calculations were carried out using the Amber* force field within MACROMODEL 5.5, employing the GB/SA solvent model for chloroform.^[26]

Synthesis: Compounds **1**, **3**, **5–9** were synthesised according to our published procedures.^[8]

Tetrabutylammonium bis(3,5-di-*tert*-butyl)phenyl phosphate (Phos): A stirred solution of the corresponding acid, bis(3,5-di-*tert*-butyl)phenyl phosphoric acid^[27] (75 mg, 0.158 mmol) in dry methanol (0.5 mL) was treated with tetrabutylammonium hydroxide (1.0 M solution in MeOH, 0.158 mL, 0.158 mmol) under argon atmosphere. The mixture was stirred for 4 h at room temperature, and then the solvent was evaporated under reduced pressure and the solid residue was dried under high vacuum over P₂O₅ at 40 °C. The tetrabutylammonium salt (**Phos**) thus obtained was stored under anhydrous conditions (113 mg, 100%). ¹H NMR (200 MHz, 26 °C, CDCl₃): δ = 7.13 (s, 1H; H_{arom}), 6.97 (s, 1H; H_{arom}), 3.37 (m, 2H; CH₂), 1.64 (m, 2H; CH₂), 1.39 (m, 2H; CH₂), 1.25 (s, 36H; *t*Bu), 0.95 (t, ³J(H,H) = 7.2 Hz, 3H; CH₃); ¹³C NMR (200 MHz, 26 °C, CDCl₃): δ = 153.7 (C-3, C-5), 151.0 (C-1), 116.0 (CH-4), 114.8 (CH-2, CH-6), 58.9 (CH₂), 34.8 (C_q of *t*Bu), 31.5 (CH₃ of *t*Bu), 24.2, 19.8 (CH₂), 13.9 (CH₃); MS (ES⁺): *m/z* (%): 959 (51) [M+NBu₄]⁺, 242 (100) [NBu₄]⁺; MS (ES⁻): *m/z* (%): 474 (41) [M-NBu₄]⁻.

1,6-Anhydro-2-benzoyl-3-deoxy-3-palmitylcarboxamide-β-D-glucopyranose (2): A mixture of **1** (20 mg, 0.05 mmol) and Bu₂SnO (12.5 mg, 0.05 mmol) in toluene (3 mL) was heated under microwave irradiation until the Bu₂SnO had completely dissolved. After cooling to room temperature, BzCl (5.8 μL, 0.05 mmol) was added. After the solution had been stirred at room temperature for 3 h, TLC analysis showed that some starting material remained. Further BzCl (4.0 μL, 0.03 mmol) was added and the reaction mixture was stirred for a further 24 h without noticeable change. The solvent was then evaporated under reduced pressure and the residue was subjected to flash column chromatography (silica; hexane/acetone 2:1) to give the desired 2-benzoyl product (**2**) (8 mg, 32%), accompanied by the 4-benzoyl isomer (6 mg, 24%) and starting material (**1**) (5 mg, 25%). (**2**): [α]_D²⁵ = +8.0 (c = 0.25 in chloroform); ¹H NMR (200 MHz, 26 °C, CDCl₃): δ = 8.06 (d, ³J(H,H) = 8.2 Hz, 2H; H_{arom}), 7.61 (t, ³J(H,H) = 7.4 Hz, 1H; H_{arom}), 7.46 (dd, ³J(H,H) = 8.2 Hz, ³J(H,H) = 7.4 Hz, 2H; H_{arom}), 6.28 (d, ³J(H_{NH},H₃) = 6.2 Hz, 1H; NH), 5.62 (s, 1H; H-1), 4.83 (d, ³J(H₂,H₃) = 3.2 Hz, 1H; H-2), 4.64 (d, ³J(H₅,H_{6-exo}) = 5.0 Hz, 1H; H-5), 4.12 (m, 1H; H-3), 4.06 (d, ³J(H_{OH},H₄) = 6.4 Hz, 1H; OH-4), 3.96 (d, ³J(H_{6-endo},H_{6-exo}) = 7.7 Hz, 1H; H-6_{endo}), 3.81 (dd, ³J(H_{6-exo},H₅) = 5.0 Hz, ³J(H,H) = 7.7 Hz, 1H; H-6_{exo}), 3.65 (broad signal, 1H; H-4), 2.21 (t, ³J(H_{CH₂},H_{CH₂}) = 7.2 Hz, 2H; CH₂CON), 1.25 (s, 24H; CH₂-hexadecyl), 0.88 (t, ³J(H_{CH₃},H_{CH₂}) = 6.2 Hz, 3H; CH₃); ¹³C NMR (200 MHz, 26 °C, CDCl₃): δ = 173.8 (CO), 164.2 (CO), 133.8, 129.9, 128.6, 126.0 (C-arom), 128.5, 102.1 (C-1), 78.4, 74.3, 71.2, 64.9, 53.9 (C-2, C-3, C-4, C-5, C-6), 33.8, 31.9, 29.7, 29.7, 29.5, 29.4, 25.1, 22.7 (CH₂-hexadecyl), 14.1 (CH₃); MS (ES⁺): *m/z* (%): 527 (100) [M+Na]⁺, 505 (69) [M+H]⁺; elemental analysis calcd (%) for C₂₉H₄₅NO₆ (503.67): C 69.15, H 9.01, N 2.78; found: C 69.30, H 9.06, N 2.81.

1,6-Anhydro-2-deoxy-2-(*N*-methyl-palmitylcarboxamide)-β-D-glucopyranose (4): NaH (2.45 mg, 0.102 mmol) was added to a stirred solution of 1,6-anhydro-2-deoxy-3,4-di-*O*-benzyl-2-(palmitylcarboxamide)-β-D-glucopyranose^[8] (20 mg, 0.034 mmol) in DMF (2 mL) under argon. After 15 min at room temperature, the mixture was treated with CH₃I (11 μL, 0.170 mmol) and stirred for a further 2 h. The solvent was then evaporated under reduced pressure, the residue was redissolved in diethyl ether, and the resulting solution was washed with saturated aqueous NH₄Cl to eliminate traces of DMF. The organic phase was dried (Na₂SO₄), filtered, and the solvent was evaporated. Without further purification, the resulting bis-*O*-benzyl-*N*-methyl amide (20.4 mg, 100%) was hydrogenated (10% Pd/C, 20 wt% of product) for 1 h under H₂ atmosphere and then the mixture was filtered through Celite. The filtrate was concentrated under reduced pressure, and flash column chromatography (silica; CH₂Cl₂/CH₃OH 20:1) of the residue gave **4** (8.8 mg, 62%). [α]_D²⁵ = -0.146 (c = 0.51 in chloroform); ¹H NMR (described as a 7:3 mixture of rotamers, 200 MHz, 26 °C, CDCl₃): δ = 5.31 (s, 0.7H; H-1), 5.32 (s, 0.3H; H-1), 4.26 (d, ³J(H₅,H_{6-exo}) = 5.4 Hz, 1H; H-5), 4.27 (d, ³J(H₂,H₃) = 6.2 Hz, 1H; H-2), 3.93 (d, ³J(H_{6-endo},H_{6-exo}) = 7.4 Hz, 0.7H; H-6_{endo}), 3.86 (d, ³J(H_{6-endo},H_{6-exo}) = 7.0 Hz, 0.3H; H-6_{endo}), 3.71–3.56 (m, 3H; H-3, H-4, H-6_{exo}), 3.08 (s, 2.1H; CH₃N), 2.90 (s, 0.9H; CH₃N), 2.35 (t, ³J(H_{CH₂},H_{CH₂}) = 7.5 Hz, 2H; CH₂CON), 1.25 (s, 26H; CH₂-hexadecyl), 0.88 (t, ³J(H_{CH₃},H_{CH₂}) = 6.5 Hz, 3H; CH₃); ¹³C NMR (200 MHz, 26 °C, CDCl₃): δ = 173.0 (CO), 101.7 (C-1), 75.6 (C-5), 72.5, 71.0 (C-3, C-4), 67.4 (C-3), 60.5 (C-2), 33.9 (CH₂CON), 31.9 (CH₃N), 29.7, 29.5, 29.5, 29.4, 29.4, 24.9, 22.7 (CH₂-hexadecyl), 14.1 (CH₃); MS (ES⁺): *m/z* (%): 414 (100) [M+H]⁺, 436 (33) [M+Na]⁺; elemental analysis calcd (%) for C₂₃H₃₅NO₅ (413.59): C 66.79, H 10.48, N 3.39; found: C 66.65, H 10.45, N 3.43.

Acknowledgements

Financial support of this work was provided by the DGES (Grant BQU2000-1501-COI) and a European TMR project (FMRX-CT98-0231). M.L.P. and E.M. are grateful to the Comunidad Autonoma de Madrid for a postgraduate fellowship and a technical fellowship, respectively.

- [1] E. J. Rohr, *Bioorganic Chemistry: Models and Applications*, Vol. 184, Springer, Berlin, 1997.
- [2] a) S. Walker, J. Murnick, D. Kahne, *J. Am. Chem. Soc.* **1993**, *115*, 7954–7961; b) G. Bifulco, A. Galeone, L. Gomez-Paloma, K. C. Nicolaou, W. J. Chazin, *J. Am. Chem. Soc.* **1996**, *118*, 8817–8824.
- [3] a) H. Pelmore, G. Eaton, M. C. R. Symons, *J. Chem. Soc. Perkin Trans. 2* **1992**, 149–150; b) A. G. Krishna, D. Balasubramanian, K. N. Ganesh, *Biochem. Biophys. Res. Commun.* **1994**, *202*, 204–210; c) H. A. Tajmir-Riahi, M. Naoui, S. Diamantoglou, *J. Biomol. Struct. Dynamics* **1994**, *12*, 217–231.
- [4] For hydroxyl–phosphate binding, see: a) S. Anderson, U. Neidlein, V. Gramlich, F. Diederich, *Angew. Chem.* **1995**, *107*, 1722–1715; *Angew. Chem. Int. Ed. Engl.* **1995**, *34*, 1596–1600; b) J. M. Coterón, F. Hackett, H.-J. Schneider, *J. Org. Chem.* **1996**, *61*, 1429–1435; c) M. Hendrix, P. B. Alper, E. S. Priestley, C.-H. Wong, *Angew. Chem.* **1997**, *109*, 119–122; *Angew. Chem. Int. Ed. Engl.* **1997**, *36*, 95–98; d) G. Das, A. D. Hamilton, *Tetrahedron Lett.* **1997**, *38*, 3675–3678.
- [5] a) K. M. Depew, S. M. Zeman, S. H. Boyer, D. J. Denhart, N. Ikemoto, S. J. Danishefsky, D. M. Crothers, *Angew. Chem.* **1996**, *108*, 2972–2975; *Angew. Chem. Int. Ed. Engl.* **1996**, *35*, 2797–2801; b) K. Toshima, R. Takano, Y. Maeda, M. Suzuki, A. Asai, S. Matsumura, *Angew. Chem.* **1999**, *111*, 3953–3955; *Angew. Chem. Int. Ed. Engl.* **1999**, *38*, 3733–3735; c) H. Xuereb, M. Maletic, J. Gildersleeve, I. Pelczar, D. Kahne, *J. Am. Chem. Soc.* **2000**, *122*, 1883–1890.
- [6] M. López de la Paz, C. González, C. Vicent, *Chem. Commun.* **2000**, 411–412.
- [7] a) M. López de la Paz, J. Jiménez-Barbero, C. Vicent, *Chem. Commun.* **1998**, 465–466; b) F. J. Luque, J. M. López, M. López de la Paz, C. Vicent, M. Orozco, *J. Phys. Chem.* **1998**, *102*, 6690–6696.
- [8] M. López de la Paz, G. Ellis, M. Pérez, J. Perkins, J. Jiménez-Barbero, C. Vicent, *Eur. J. Org. Chem.* **2002**, 840–855.
- [9] Molecular mechanics calculations were carried out using Amber* within MACROMODEL 5.5, employing the GB/SA solvent model for CHCl₃. We have modelled both possible bidentate phosphate complexes involving OH-2 and OH-4, and that involving OH-4 and NH-3 of sugar **1**. According to the steric energy values, the second one is more stable.
- [10] Neither the sugar nor the phosphate dimerises in chloroform solution under the conditions used for the titration.
- [11] Downfield shifts of the OH and NH resonances, accompanied by upfield shifts of the CH resonances, allowed us to measure the *K_a* values. All stability constants were measured in triplicate and the Δ*G*[°] values were found to be reproducible to within ±0.1 kcal mol⁻¹. We thank Prof. C. Hunter (University of Sheffield) for kindly providing the fitting program.
- [12] Compound **6** is an exception. It forms a 1:2 complex (**6-Phos**).
- [13] The *K_a* value that we obtained for monoalcohol **8-Phos** complex, 1.9 M⁻¹, is of the same order as those measured by Schneider for aliphatic monohydroxyl compounds.^[4b]
- [14] a) E. S. Stevens, N. Sugawara, G. M. Bonora, C. Toniolo, *J. Am. Chem. Soc.* **1980**, *102*, 7048–7050; b) C. Huang, L. A. Cabell, V. Lynch, E. V. Anslyn, *J. Am. Chem. Soc.* **1992**, *114*, 1900–1901.
- [15] Mixing time for **1** (600 ms, 299 K), and **1-Phos** (600 ms, 299 K). NOEs between the aromatic resonances (H2 and H5) of the phosphate and the alkyl methyl and methylene resonances of the ammonium salt confirmed the presence of the ionic pair.
- [16] IR spectra were recorded from dilute solutions in a fixed pathlength (0.1 mm) liquid cell with KBr windows. The spectra of **Phos**, the sugars, and the sugar–**Phos** complexes were ratioed to the background spectrum recorded with dry CH₂Cl₂ in the IR cell.
- [17] For sugar **2**, the intermolecular association bands in the range 3400–3100 cm⁻¹ are observed only very weakly as compared with those of

the complex **1-Phos**, which is to be expected considering the low saturation obtained for **2-Phos** under these experimental conditions. For this reason, the observations in the region of the amide modes in **2** are inconclusive. However, by normalizing the spectra with respect to the intensity of the band due to the ester carbonyl group of the OBz moiety, a very slight reduction in the relative intensity of the amide II mode, characteristic of the NH bond, can be observed on going from **2** to **2-Phos**.

- [18] a) G. A. Jeffrey, W. Saenger, *Hydrogen Bonding in Biological Structures*, Springer, Berlin, **1991**; b) H. Kleeberg, D. Klein, W. A. P. Luck, *J. Phys. Chem.* **1987**, *91*, 3200–3203; c) G. Maes, J. Smets, *J. Phys. Chem.* **1993**, *97*, 1818–1825.
- [19] B. N. Craig, M. U. Janssen, B. M. Wichersham, D. M. Rabb, P. S. Chang, D. J. O’Leary, *J. Org. Chem.* **1996**, *61*, 9610–9613.
- [20] 3J analysis of the 1H NMR spectra showed that all the compounds other than **4** exhibit 3J values consistent with the adoption of a chair conformation in $CDCl_3$ and $CDCl_3/CCl_4$ solution: A. Rivera-Sagredo, J. Jiménez-Barbero, *Carbohydr. Res.* **1991**, *215*, 239–250.
- [21] NMR (CIS and temperature coefficients) and IR structural data (see above) confirmed the non-involvement of the amide in complexation.
- [22] The C2–NHCO bond rotation is more restricted than that about C2–OH. We cannot rule out the presence of a percentage of the H-bonded isomer in solution ($O-H4 \rightarrow O-H2$), which will be shifted upon binding to the favored H-bonding isomer ($O-H2 \rightarrow O-H4$).
- [23] Based on the study of Williams,^[24] we have plotted the calculated limiting chemical shifts of the NH resonance at saturation for **1-Phos** and **2-Phos** in both solvent systems. The larger binding shift of the NH in **1** as compared to that in **2** is taken to imply stronger interaction with **Phos**. It emerged that the intermolecular NH–**Phos** H-bond in **1-Phos** is cooperatively enhanced by the presence of a neighbouring interaction (the intramolecular H-bond) as compared to the same H-bonding motif in **2-Phos** (Figure 2). The same holds true for the OH-4 resonance of **1-Phos** compared to that of **2-Phos** in the two media.
- [24] M. S. Searle, M. S. Westwell, D. H. Williams, *J. Chem. Soc. Perkin Trans. 2* **1995**, 141–151.
- [25] H. Adams, F. J. Carver, C. A. Hunter, J. C. Morales, E. M. Seward, *Angew. Chem.* **1996**, *108*, 1628–1631; *Angew. Chem. Int. Ed. Engl.* **1996**, *35*, 1542.
- [26] W. C. Still, A. Tempczyk, R. C. Hawley, T. Hendrickson, *J. Am. Chem. Soc.* **1990**, *112*, 6127–6129.
- [27] The acid was prepared from the corresponding methyl ester.^[28]
- [28] A. C. Hengge, W. W. Cleland, *J. Am. Chem. Soc.* **1991**, *113*, 5835–5841.

Received: October 15, 2001 [F3615]